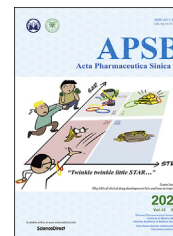




Chinese Pharmaceutical Association  
Institute of Materia Medica, Chinese Academy of Medical Sciences

Acta Pharmaceutica Sinica B

[www.elsevier.com/locate/apsb](http://www.elsevier.com/locate/apsb)  
[www.sciencedirect.com](http://www.sciencedirect.com)



ORIGINAL ARTICLE

# Screening potential P-glycoprotein inhibitors by combination of a detergent-free membrane protein extraction with surface plasmon resonance biosensor



Yuhong Cao<sup>a,b,†</sup>, Jiahao Fang<sup>a,†</sup>, Yiwei Shi<sup>a</sup>, Hui Wang<sup>a</sup>,  
Xiaofei Chen<sup>a</sup>, Yue Liu<sup>a</sup>, Zhenyu Zhu<sup>a</sup>, Yan Cao<sup>a,\*</sup>,  
Zhanying Hong<sup>a,\*</sup>, Yifeng Chai<sup>a</sup>

<sup>a</sup>School of Pharmacy, Second Military Medical University, Shanghai Key Laboratory for Pharmaceutical Metabolites Research, Shanghai 200433, China

<sup>b</sup>Zhejiang Institute for Food and Drug Control, Hangzhou 310057, China

Received 27 December 2021; received in revised form 3 March 2022; accepted 21 March 2022

## KEY WORDS

Styrene maleic acid;  
P-Glycoprotein;  
Surface plasmon resonance;  
Membrane proteins;  
Inhibitor screening;  
Affinity calculation;  
Natural products;  
Multidrug resistance

**Abstract** P-glycoprotein (P-gp) highly expressed in cancer cells can lead to multidrug resistance (MDR) and the combination of anti-cancer drugs with P-gp inhibitor has been a promising strategy to reverse MDR in cancer treatment. In this study, we established a label-free and detergent-free system combining surface plasmon resonance (SPR) biosensor with styrene maleic acid (SMA) polymer membrane proteins (MPs) stabilization technology to screen potential P-gp inhibitors. First, P-gp was extracted from MCF-7/ADR cells using SMA polymer to form SMA liposomes (SMALPs). Following that, SMALPs were immobilized on an SPR biosensor chip to establish a P-gp inhibitor screening system, and the affinity between P-gp and small molecule ligand was determined. The methodological investigation proved that the screening system had good specificity and stability. Nine P-gp ligands were screened out from 50 natural products, and their affinity constants with P-gp were also determined. The *in vitro* cell verification experiments demonstrated that tetrandrine, fangchinoline, praeruptorin B, neobaicalein, and icariin could significantly increase the sensitivity of MCF-7/ADR cells to Adriamycin (Adr). Moreover, tetrandrine, praeruptorin B, and neobaicalein could reverse MDR in MCF-7/ADR cells by inhibiting the function of P-gp. This is the first time that SMALPs-based stabilization strategy was applied to SPR analysis system. SMA polymer can retain P-gp in the environment of natural lipid bilayer and thus maintain the correct conformation and physiological functions of P-gp. The developed system can quickly and

\*Corresponding authors. Tel.: +86 21 81871269 (Zhanying Hong), Tel/fax: +86 21 81871331 (Yan Cao).

E-mail addresses: [caoyan@smmu.edu.cn](mailto:caoyan@smmu.edu.cn) (Yan Cao), [hongzhy001@163.com](mailto:hongzhy001@163.com) (Zhanying Hong).

<sup>†</sup>These authors made equal contributions to this work.

<https://doi.org/10.1016/j.apsb.2022.03.016>

2211-3835 © 2022 Chinese Pharmaceutical Association and Institute of Materia Medica, Chinese Academy of Medical Sciences. Production and hosting by Elsevier B.V. This is an open access article under the CC BY-NC-ND license (<http://creativecommons.org/licenses/by-nc-nd/4.0/>).

accurately screen small molecule ligands of complex MPs and obtain affinity between complex MPs and small molecule ligands without protein purification.

© 2022 Chinese Pharmaceutical Association and Institute of Materia Medica, Chinese Academy of Medical Sciences. Production and hosting by Elsevier B.V. This is an open access article under the CC BY-NC-ND license (<http://creativecommons.org/licenses/by-nc-nd/4.0/>).

## 1. Introduction

Surface plasmon resonance (SPR) is a label-free biomolecular interaction strategy, which can measure the membrane proteins (MPs)–ligand interaction and can characterize the interaction between a pair of soluble binding molecules in detail<sup>1,2</sup>. SPR has now become a powerful tool for drug screening and is currently applied to new drug discovery, as it can determine affinity between molecules quickly. The premise of SPR applications is that purified protein must be immobilized on the biosensor's surface. Unfortunately, MPs are difficult to be purified and immobilized on the biosensor's surface since their complex structures require a lipid environment to maintain their correct conformation<sup>3</sup>.

MPs play an important role in intercellular communication, material transfer and energy conversion. However, it is difficult to maintain their activity when they are separated from the cell membrane environment<sup>4–6</sup>. Purifying MPs is time-consuming and laborious, and it is difficult to obtain complex MPs. However, in order to enable rapid and quantitative analysis of ligand–MP interactions, these interactions must be probed in lipid bilayers that resemble their native membrane environment<sup>7,8</sup>. Therefore, a method that immobilizes MPs together with their lipid environment on the biosensor's surface in SPR analysis would be an advantageous tool for discovering new drugs<sup>9</sup>. To interface with existing SPR instrumentation, MPs can be immobilized as detergent “solubilized” protein, deposited in supported lipid bilayers, or trapped in vesicles and are subsequently captured. Some technologies are gradually being developed, including liposomes, double cells and discs strategies to provide a membranous natural environment for MPs to be presented in natural or near natural form<sup>3,10</sup>. However, these techniques based on detergent solubility require optimization of detergent properties and concentrations, which can cause a loss to protein activity in the process of recombination.

In previous studies, we employed lentiviruses particles (LVPs) to stabilize P-glycoprotein (P-gp) and CXC chemokine receptor 4 (CXCR4), and immobilized LVPs on the surface of CM5 chip for screening small molecular ligands<sup>11,12</sup>. LVPs can serve as a natural environment for MPs, omitting complex purification steps. However, there are thousands of receptors on the outer membrane of LVPs, so the environment of target MPs is different from that of mammalian cells, resulting in the low specificity and poor accuracy of screening results.

In recent years, styrene maleic acid (SMA) polymer is more and more widely used in the extraction and purification of MPs. SMA can realize self-assembly in cell membrane: SMA ring surrounds lipids, forms a disk-shaped structure of layered membrane, and produces very uniform particles with a diameter of 9 to 20 nm<sup>13,14</sup>. The advantage of SMA over detergents and artificial

membranes is that it extracts the target protein into SMA lipid particles (SMALPs) by recognizing the spontaneous assembly of endogenous lipids around the target protein, and the protein is thus retained in the environment of natural lipid bilayer. In addition, MPs extracted into SMALPs show significant stability compared with detergent and artificial membrane, and have successfully been used for both functional and structural studies<sup>15,16</sup>. So far, SMA polymers have been used to stabilize the dissolution of many MPs, including AcrB<sup>17</sup>, ATP-binding cassette (ABC) transporter such as MRP<sup>18</sup>, potassium channel KcsA<sup>19</sup>, penicillin-binding protein PBP2A<sup>20</sup> and adenosine A2A receptor<sup>21</sup>.

ABC transporters such as P-gp are responsible for conferring multidrug resistance (MDR) phenotype, which first become evident during treatment of cancers with anti-cancer drugs<sup>22,23</sup>. The combination of anti-cancer drugs with P-gp inhibitors has been a promising strategy to reverse MDR in cancer treatment. However, to date, no compound has demonstrated a significant reversal of MDR without causing considerable toxicity<sup>24</sup>. Due to ABC transporters' low expression level and hydrophobic properties in cells, the requirement for a lipid double-layer environment to maintain their correct conformation makes expression, extraction, and purification more difficult in the study of function and structure<sup>25</sup>. Therefore, pure ABC transporters are difficult to acquire, and the screening of their ligands is mainly based on cell bidirectional transport experiments and computer-assisted virtual screening<sup>26–28</sup>. Currently, researchers have applied SMA technology to extract and stabilize ABC transporters in insect cell membranes, and they have discovered that MPs can maintain their correct conformation and physiological functions when stabilized by SMA<sup>18</sup>. However, applying SMA technology to extract and stabilize complex MP such as P-gp, and then studying the interaction between ligands and MPs supported in SMA has not yet been reported.

In this study, an SMA-based MPs immobilization strategy was developed and combined with SPR biosensor analysis to present a novel approach for screening potential P-gp inhibitors. SMA was utilized to extract P-gp in MCF-7 and MCF-7/ADR cells to obtain SMALPs-P-gp. P-gp was stabilized in endogenous lipids and then employed in SPR technology to study its interaction with small molecules. To the best of our knowledge, this is the first time that an SMA strategy for stabilizing MPs is combined with SPR analysis and the method shows high efficiency in screening potential P-gp inhibitors. It can not only perform effective compound screening but also accurately determine the affinity between compounds and MPs. SMA polymer strategy can solve the problems in the field of MPs determination, expand the scope of SPR application, and provide the possibility for MPs–drugs interactions and the development of MPs-targeted drugs.

## 2. Materials and methods

### 2.1. Chemicals and reagents

Styrene maleic anhydride co-polymer SMA2000 was purchased from Cray Valley (France). BCA Protein Assay Kit and Cell Counting Kit-8 (CCK-8) were purchased from Beyotime (Shanghai, China). All standard compounds were purchased from Standard Technology Co. (Shanghai, China). Materials and reagents used for SPR assays (including CM5 chips, EDC, NHS and ethanolamine) were purchased from GE Healthcare (Shanghai, China). P-gp ELISA Kit was purchased from Enzyme-linked Biotechnology Co. Ltd. (Shanghai, China). Trans-well filters were purchased from Corning Costar (Cambridge, MA, USA). Rh-123 was purchased from the Sigma Chemical Co. (St. Louis, MO, USA), and RPMI 1640 and fetal calf serum and 0.25% trypsin were purchased from Corning Costar (Cambridge, MA, USA). Rabbit anti-P-gp antibody (ab170904), rabbit anti-GAPDH antibody (ab181603), HRP conjugated goat anti-rabbit IgG (H + L) and HRP conjugated goat anti-mouse IgG (H + L) for Western blot were purchased from Abcam (USA). P-Glycoprotein Monoclonal Antibody (C494) and mouse anti-P-gp antibody (MA1-26529) were purchased from Thermo Fisher Scientific (Waltham, MA, USA).

### 2.2. Cell lines and culture conditions

MCF-7 and MCF-7/ADR cell lines were purchased from Shanghai Xinyu Biological Technology Co., Ltd. (Shanghai, China). MCF-7 and MCF-7/ADR cells were cultured in RPMI 1640 containing 10% (v/v) fetal bovine serum and 1000 µg/mL glutamine. Additionally, 1000 ng/mL adriamycin (Adr) was added to the MCF-7/ADR cells. MDR1-transfected Medin-Darby Canine Kidney cell lines (MDCK-MDR1) were kindly provided by Dr. Zeng (Zhejiang University, China). MDCK-MDR1 cells were cultured in Dulbecco's modified eagle's medium containing 10% (v/v) fetal bovine serum and two antibiotics (100 µg/mL streptomycin and 100 U/mL penicillin). All cells were cultured at 37 °C in 5% CO<sub>2</sub>.

### 2.3. Preparation of styrene maleic acid co-polymer

The commercially available polymers are provided as styrene maleic anhydride co-polymer and need to be converted into styrene maleic acid co-polymer by hydrolysis using NaOH. 25 g of styrene maleic anhydride co-polymer (SMA2000) was dissolved in 250 mL of 1 mol/L NaOH in a round bottom flask and stirred for 24 h at room temperature, then the round bottom flask was heated and boiled until all the solids were dissolved. After the solution cooled at room temperature, the pH was adjusted to < 5 by adding concentrated hydrochloric acid in a fume hood and stirred evenly. 1 mL of concentrated hydrochloric acid was needed for every 6 mL of polymer solution generally and the copolymer began to precipitate. The precipitate was washed five times with water followed by separation using centrifugation. After the last washing, 60 mL of 0.6 mol/L NaOH was added to the precipitate and the pH was adjusted to 8.0. The SMA copolymer was freeze-dried and stored at room temperature.

### 2.4. Preparation of cell membrane from MCF-7 cells and MCF-7/ADR cells

The cells were washed twice with PBS and were thus gently scraped off by adding PBS containing protease inhibitor. The cells were disrupted by ultrasound, and the suspension was centrifuged at 1000×g for 10 min. The supernatant was centrifuged at 20,000×g for 60 min. The pellet was re-suspended in PBS containing protease inhibitor, and aliquots of the pellet suspension were then stored at −80 °C. Except for special instructions, all operations were performed at 4 °C.

### 2.5. Preparation of SMALPs

Membranes were pelleted (100,000×g, 20 min, 4 °C), then suspended in PBS at a final concentration of 80 mg/mL membrane (wet membrane mass) and SMA was then added to a final concentration of 2.5% (w/v). Samples were incubated at room temperature with gentle shaking for 4 h. Insoluble material was removed by centrifugation (100,000×g, 20 min, 4 °C), and the supernatant was taken containing liposomes SMALPs-MCF-7 and SMALPs-MCF-7/ADR, respectively. The collected SMALPs were concentrated with an ultrafiltration tube (100 kDa), and the protein was quantified using the BCA Protein Assay Kit. The SMALPs liposomes were stored at −80 °C.

### 2.6. Experimental conditions for P-gp-SMALPs-SPR analysis

The cells were broken by ultrasonic disruption to obtain cell membrane.  $2 \times 10^7$  MCF-7/ADR cells were broken at a constant power of 600 W with a pulse for 2 s on and 10 s off as one cycle, and processed 5, 10, 15 and 20 cycles, respectively. Membranes were pelleted (100,000×g, 20 min, 4 °C), then suspended in PBS at a final concentration of 80, 160, 320 and 640 mg/mL (wet membrane mass) and SMA was then added to a final concentration of 2.5% (w/v). Sample were gently shaken at room temperature for 1, 2, 4 and 24 h treatment, respectively. After SMA extraction, Western blot experiment and ELISA experiment were used to analyze the extraction efficiency of P-gp.

### 2.7. Coupling time of SMALPs on L1 chip

The L1 chip was chosen for SMALPs coupling with non-covalently bound to the lipophilic group on the L1 chip's surface. The total protein concentration in SMALPs was quantified by BCA assay. The SMALPs of the same concentration were coupled on the chip for 30 min one time, the flow rate was 2 µL/min, and the coupling time was continuously increased to 3 h for 6 times. The RU value was used to determine the highest saturation of SMALPs on the L1 chip.

### 2.8. Characterization of the SMALPs-L1 chip's specificity and activity

The SMALPs obtained from MCF-7 cells were immobilized on FC 1 cell used as reference FC and SMALPs obtained from MCF-7/ADR cells were immobilized on FC 2 cell used as active FC, respectively. The flow rate was 2 µL/min, the reaction time was 30 min. P-gp inhibitors valsopodar and verapamil were selected as

positive drugs, dexamethasone as negative drugs, and P-gp specific antibodies (C494) were used to evaluate the specificity and activity of SMALPs-L1 chip. In the process, the signal of reference FC is deducted from the signal of active FC, and then the signal of ligand acting on P-gp was acquired because the influence of other proteins was excluded from the analysis. The flow rate of ligands was 10  $\mu\text{L}/\text{min}$ , the binding time was 60 s, and the dissociation time was 30 s.

### 2.9. Characterization of the SMALPs-L1 chip's stability

The coupling time and the stability of the SMALPs on the chip were characterized to ensure the accuracy of this method. The SMALPs were coupled to the L1 chip at a flow rate of 2  $\mu\text{L}/\text{min}$  and the baseline was recorded RU for 6, 12, 24, 48, and 72 h. P-gp inhibitor valsopodar was used as the positive drug to evaluate the activity of SMALPs-L1 chip by affinity verification.

### 2.10. Determination of protein concentration and the size of SMALPs

#### 2.10.1. ELISA

Enzyme-linked immunosorbent assay (ELISA) was used to determine the P-gp content according to the kit operating procedures. The steps of mixing with the antibody, incubating at a constant temperature, washing the plate, reacting with the substrate, and terminating the reaction were carried out successively. Standard wells, blank wells and sample wells were set as required. Within 15 min after terminating the reaction, the absorbance (OD value) of each well was measured at the wavelength of 450 nm and the sample concentration was thus calculated.

#### 2.10.2. Western blots

Proteins were analyzed by SDS-PAGE and Western blot using specific antibodies. SMALPs were analyzed in Western blot with anti-GAPDH (1:3000) mAb, and anti-P-gp (1:2000) mAb. Equal volume of lysate was added to SMALPs sample for 30 min. After the lysis was completed, the sample was centrifuged for 10 min at  $12,000\times g$  and the total protein of the liquid was detected by BCA method. Samples containing 20  $\mu\text{g}$  of protein were subjected to 10% SDS-PAGE and electro-transferred to nitrocellulose membranes. Membranes were blocked with 5% non-fat milk/0.05% Tween PBS, incubated with primary antibodies against P-gp and GAPDH overnight. The blot was washed and incubated for 2 h at room temperature with HRP conjugated Goat anti-Rabbit IgG (H + L) (1:5000) and HRP conjugated Goat anti-Mouse IgG (H + L) (1:5000) separately. The blots were then analyzed by scanning densitometry using an Odyssey Infrared Imaging System (Li-cor, USA).

#### 2.10.3. TEM

Transmission electron microscopy (TEM) was used to characterize the size and shape of SMALPs. Since SMA would interfere with the view of TEM, it was necessary to remove the residual SMA in the sample. SMALPs were separated using AKTA Pure system (GE Healthcare) and Superdex 200 10/300 GL column (GE Healthcare) to remove the residual SMA. The buffer was PBS and the flow rate was 0.5 mL/min. The SMALPs fraction was collected and concentrated to 0.5 mL (10 kDa, Merck) with an

ultrafiltration tube. The SMALPs were adsorbed onto a carbon-coated grid, the excess solution was blotted dry, and the sample was negatively stained with uranyl acetate [2% (w/v), 30 s]. JEM 100CX (JEOL) electron microscope records electron micrographs at 50,000 times magnification under 100 kV. A lextight X5 scanner (Hasselblad) was used to process the micrographs.

### 2.11. Establishment of P-gp-SMALPs-SPR screening system

According to the optimized conditions, the SMALPs-MCF-7 were immobilized on FC 1 of the L1 chip, while the SMALPs-MCF-7/ADR were immobilized on FC 2 of the L1 chip, and the affinity between the compounds and the protein on the chip was obtained by subtracting the signal values on the two FCs. The target compounds which had a response signal on the surface of the chip was performed affinity verification consequently. Thus, the P-gp-SMALPs-SPR system was established to screen active compounds to reverse P-gp-mediated MDR.

### 2.12. Screening P-gp potential inhibitors from natural products

Standard compounds were diluted in 5% DMSO PBS (32  $\mu\text{mol}/\text{L}$ ) and injected into different channels of the chip one by one at a flow rate of 10  $\mu\text{L}/\text{min}$ , and then running buffer was continuously injected for 60 s (dissociation phase). The response between the compound and P-gp was calculated by subtracting the signal values on the two FCs when the compound flew through the surface of the chip. Ligands with the response value on the detection channel higher than that on the reference channel were regarded as target compounds for further affinity verification.

### 2.13. Affinity verification

The binding kinetic information between the compound and the protein is characterized by affinity detection. Standard compounds were diluted in a series of concentrations of 5% DMSO in PBS and injected into the system at a flow rate of 10  $\mu\text{L}/\text{min}$ . The binding time was 60 s, and the dissociation time was 30 s. The FC 1 channel (immobilized SMALPs-MCF-7) was used as the FC to calibrate the sensor signal. All steps were performed using the system's automated sampling, in response to changes in the signal expressed in units (RU). Biacore T200 analysis software was used to perform overall fitting through the steady-state affinity model (1:1) to obtain the affinity constant ( $K_D$ ).

### 2.14. Activity verification of target compounds

The effects of target compounds on the  $\text{IC}_{50}$  value of Adr on MCF-7/ADR cells toward Adr were investigated to verify the activity of reversing MDR *in vitro*. Then the Western blot experiment was used to verify the effect of the target compound on the expression of P-gp, and rhodamine 123 (Rh123) transport experiment was used to verify the effect of the target compound on the function of P-gp.

#### 2.14.1. Cytotoxicity

MCF-7 and MCF-7/ADR cells were seeded into a 96-well plate at a density of  $5 \times 10^3$  cells/well. Then, the positive drugs and

target compounds of different concentrations (1.25, 2.5, 5, 10, 20, 40, 80  $\mu\text{mol/L}$ ) were incubated with MCF-7 cells and MCF-7/ADR cells for 24 h. The sensitivity of cells to positive drug and target compounds was measured as previously using the CCK8 assay<sup>29</sup>.

#### 2.14.2. The activity of reversing MDR

CCK8 analysis method was used to determine the cytotoxicity toward MCF-7/ADR induced by Adr. MCF-7/ADR cells were seeded into 96-well plates at a density of  $5 \times 10^3$  cells/well. After incubated with the target compounds for 24 h, the cells were incubated with different concentrations of Adr (0, 1.56, 3.13, 6.25, 12.5, 25, 50, 100  $\mu\text{mol/L}$ ) for 24 h. The effects of target compounds on sensitivity of cells to Adr was measured as previously using the CCK8 assay.

#### 2.14.3. Determination of P-gp expression

MCF-7/ADR cells were seeded into 6-well plates at a density of  $1 \times 10^6$  cells/well. After incubated with the target compounds for 48 h, the cells were washed three times and lysed on ice for 30 min. The cell lysate was collected and centrifuged at  $12,000 \times g$  for 10 min. The supernatant was taken for BCA quantitative detection of total protein and Western blot detection.

#### 2.14.4. Rh123 transport experiment

The efflux function of P-gp was verified by Rh123 transport experiment which performed on Transwell plates using MDCK-MDR1 cells. The transport assay was carried out as previously method<sup>30</sup>.

### 3. Results and discussion

#### 3.1. Construction of P-gp-SMALPs-SPR screening system

In this study, a novel screening system for potential P-gp inhibitors was established by combining SMA MPs stabilization strategy with SPR technology, as shown in Fig. 1. The human breast cancer cells MCF-7 and Adr-resistant breast cancer cells MCF-7/ADR with overexpressed P-gp were used as cell models. First, cell membranes were extracted from the two kinds of cell lines, and SMA polymer was added to form SMALPs-MCF-7 and SMALPs-MCF-7/ADR. SMA polymer with an extended chain conformation can interact with a portion of lipid bilayer, in which rings of elongated polymer strands encircle 100–200 lipids, allowing the hydrophobic groups to cut out a discoidal section<sup>31</sup>. The original ecological liposomes encapsulated by SMA ensure the natural membrane environment of MPs (Fig. 1A). Then the SMALPs-MCF-7 was coupled to (FC 1) as the reference FC, which was used as a control to eliminate signals from uninterested proteins on the surface of MCF-7 cells. And SMALPs-MCF-7/ADR was coupled to FC 2 as the active FC. The interaction signal of the ligand and the P-gp on the L1 chip's surface was obtained by the signal deduction of the FC 2 and FC 1, thus an effective and rapid P-gp potential inhibitor screening system was established (Fig. 1B). Two FCs were used on the SPR chip to exclude the interference from heterogeneous proteins of cell membrane. During the detection process, the signal of the reference FC was subtracted from the signal of the active FC to obtain the affinity between the compound and P-gp.

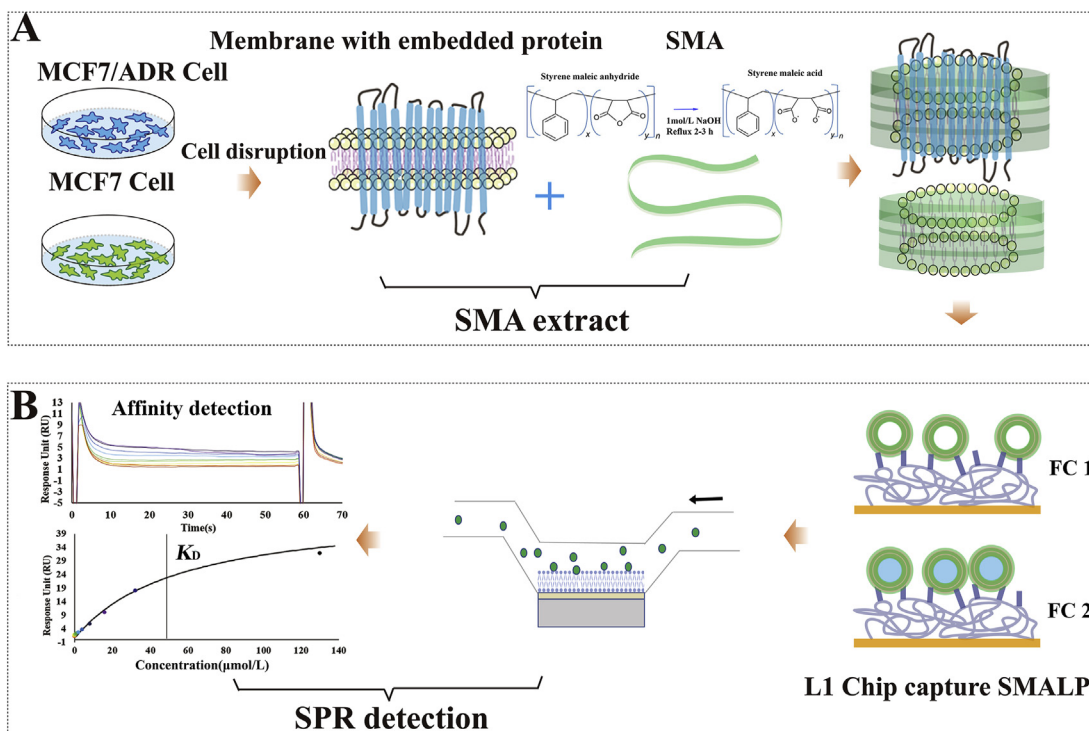


**Figure 1** Scheme of SMA polymer MPs stabilization technology combined with SPR system. (A) SMA polymer was used to extract MPs from MCF-7 cell membrane and MCF-7/ADR cell membrane, and the SMALPs were obtained. (B) The SMALPs obtained from MCF-7 cell with low P-gp expression was immobilized on FC1 of L1 sensor chip which used as a control to eliminate signals from uninterested proteins on the cell membrane of MCF-7 cells, while the SMALPs obtained from MCF-7/ADR cell with high P-gp expression was immobilized on FC2 which was used as an active FC.

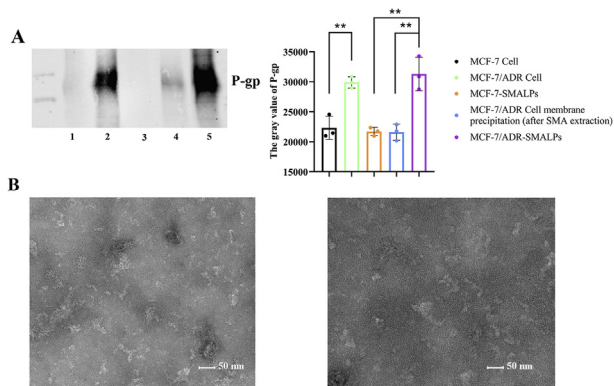


**Figure 2** The MPs extraction of MCF-7 and MCF-7/ADR cell by SMA. (A) The P-gp content of different cell membrane samples were verified by Western blot (1, MCF-7 cell lysate; 2, MCF-7/ADR cell lysate; 3, SMALPs-MCF-7; 4, MCF-7/ADR membrane precipitation after SMA extraction; 5, SMALPs-MCF-7/ADR. Data are mean  $\pm$  SD,  $n = 3$ ;  $**P < 0.01$ , MCF-7/ADR cell versus MCF-7 cell group, MCF-7-SMALPs and MCF-7/ADR cell membranes precipitation after SMA extraction versus MCF-7/ADR-SMALPs group). (B) TEM image of SMALPs particles negatively stained with uranyl acetate, SMALPs-MCF-7/ADR is shown on the left and SMALPs-MCF-7 is shown on the right, scale bar = 50 nm.

### 3.2. Extraction of P-gp using SMA

The effect of SMA on the extraction of P-gp was investigated by Western blot. The content of P-gp in cell membrane, SMALPs-MCF-7, SMALPs-MCF-7/ADR and the cell membranes pellet after SMA extraction were verified. The results are shown in Fig. 2A. It was found that P-gp was overexpressed in MCF-7/ADR cell membrane, and SMA can extract P-gp in the cell membrane. The cell membrane suspension became clear after SMA extraction, which indicated P-gp were successfully extracted.

### 3.3. Size characterization of SMALPs

Next, the morphological characterization of SMALPs was characterized by TEM. SMALPs was separated by SEC to remove excess SMA, and the purified SMALPs was collected and visualized (stained) using cryo-EM. As shown in Fig. 2B, EM analysis of negatively stained SMALPs shows dispersed disks with average diameters of 10–15 nm, and the size of SMALPs obtained by SMA extraction of cell membrane was uniform, which was consistent with literature reports<sup>13</sup>.

### 3.4. Optimization of SMA extraction

The ultrasonic time has a great impact on the degree of cell disruption, while the ratio of SMA to cell membrane and the extraction time have a great impact on the extraction efficiency of MPs. In the process of SMA extraction, the effects of ultrasonic cycles (5, 10, 15, 20), the membrane concentration (40, 80, 160, 320 mg/mL), and the incubation time with SMA (1, 2, 4, 24 h) on the extraction efficiency of MPs were investigated. A total of 16 samples were investigated by orthogonal design as shown in Table 1. The extraction efficiency was evaluated by the P-gp concentration in each SMALPs sample (Fig. 3A and B).

The results showed that the extraction efficiency of P-gp was greatly affected by the cycle numbers of ultrasound, SMA

**Table 1** The orthogonal experiment of the pretreatment for SMALPs

No.	Ultrasonic cycle	Incubation time (h)	Membrane concentration (mg/mL)
1	10	2	320
2	10	1	80
3	20	1	320
4	15	2	40
5	15	1	160
6	5	4	320
7	5	1	40
8	5	24	80
9	15	24	320
10	5	2	160
11	20	2	80
12	20	24	160
13	10	24	40
14	15	4	80
15	20	4	40
16	10	4	160

incubation time and membrane concentration. It was found that the expression of P-gp in sample 3, 5, 6, 9, 15 and 16 was higher.

The content of P-gp in the samples was further detected by ELISA (Fig. 3C). The content of P-gp in samples 3, 6, 9, 11, 12, 14, 15 and 16 was higher. Taking the results of Western blot and ELISA together, the pretreatment method of sample 15 was selected as the optimized method. In conclusion, the optimized pretreatment conditions were ultrasonic 20 times to crush cells, cell membrane concentration of 40 mg/mL, and SMA incubation time of 4 h.

### 3.5. Coupling condition of SMALPs on L1 chip

SMALPs would precipitate at acidic pH values, and the pH dependency is a potential drawback for SMA application in SPR technology. This problem can be solved by sensor chip L1 which surface consists of a carboxymethylated dextran matrix pre-immobilized with lipophilic groups for rapid and reproducible capture of lipid vesicles, and the process is not limited by pH. The binding process involves diffusion of the vesicles to the surface and incorporation of the lipophilic structures on sensor chip L1 into the lipid membrane, non-covalently anchoring the vesicle.

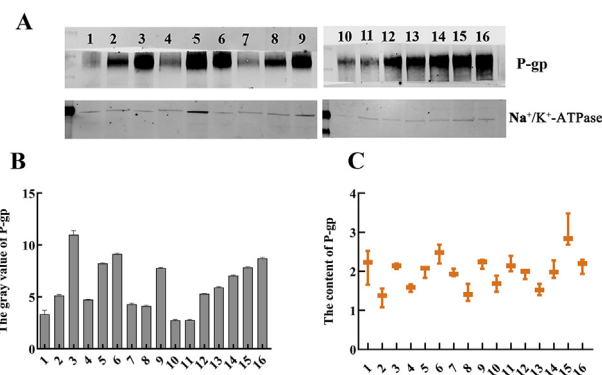


**Figure 3** The content of P-gp in samples under different pre-processing methods. (A) The Western blot results. (B) The band gray value calculated by Image J. (C) The content of P-gp detected by ELISA. Data are mean  $\pm$  SD,  $n = 3$ .

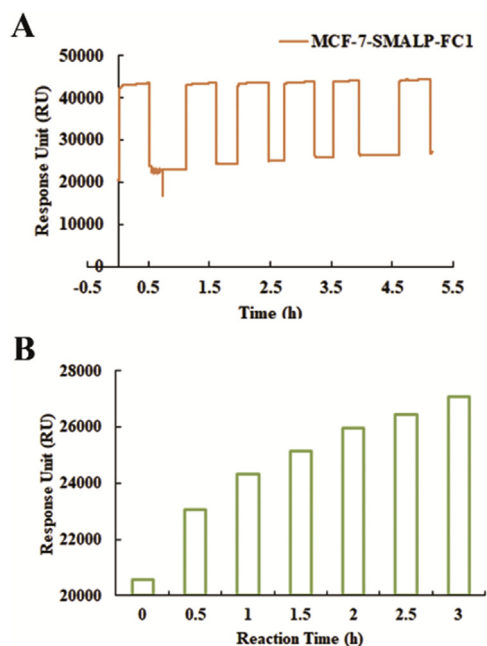


**Figure 4** The coupling condition of SMALPs on the chip. (A) Changes in response signal when the SMALPs was injected into the surface of L1 chip (B) The relationship between the amount of SMALPs coupled on the chip and the reaction time.

The coupling condition of SMALPs in a single channel of L1 chip was investigated. SMALPs-MCF-7 were injected into FC 1 of L1 chip at a flow rate of 2  $\mu\text{L}/\text{min}$ , the reaction time was continuously increased, each injection lasted for 30 min, and a total of 6 injections resulted in a total reaction time of 3 h. The baseline was about 2000 RU and the increase of the response value on the channel represented the coupling amount of SMALPs. As shown in Fig. 4A, the absolute response value of the chip rise with the increase of injection time, which indicated that the content of liposomes in the channel on the chip was increasing and the binding sites were not all reacted. The absolute response value of the chip channel after each coupling was plotted with the reaction time, as shown in Fig. 4B. With the extension of reaction time, the increase speed of liposomes on the sensor slowed down with a trend of saturation, indicating that the binding sites in the chip channel were gradually fully occupied. The maximum coupling amount was 6000 RU.

### 3.6. Specificity and activity of P-gp-SMALPs-L1 chip

P-gp inhibitors and specific C494 antibody were used to verify the feasibility and specificity of the established screening system. First, SMALPs-MCF-7 was coupled to FC 1 as a reference channel and SMALPs-MCF-7/ADR was coupled to FC 2 as detection channel to construct detection system (Fig. 5A). P-gp inhibitors valsopodar and verapamil were used as positive drugs,

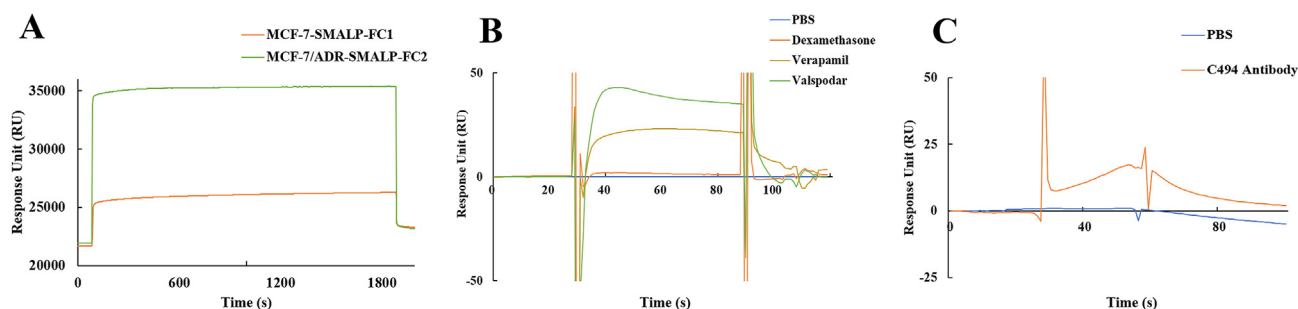


**Figure 5** The activity of SMALPs-L1 chip. (A) SMALPs-MCF-7 and SMALPs-MCF-7/ADR were coupled to different channels of the chip (B) The response of individual small molecules on the chip (C) The response of the C494 antibody on the chip.

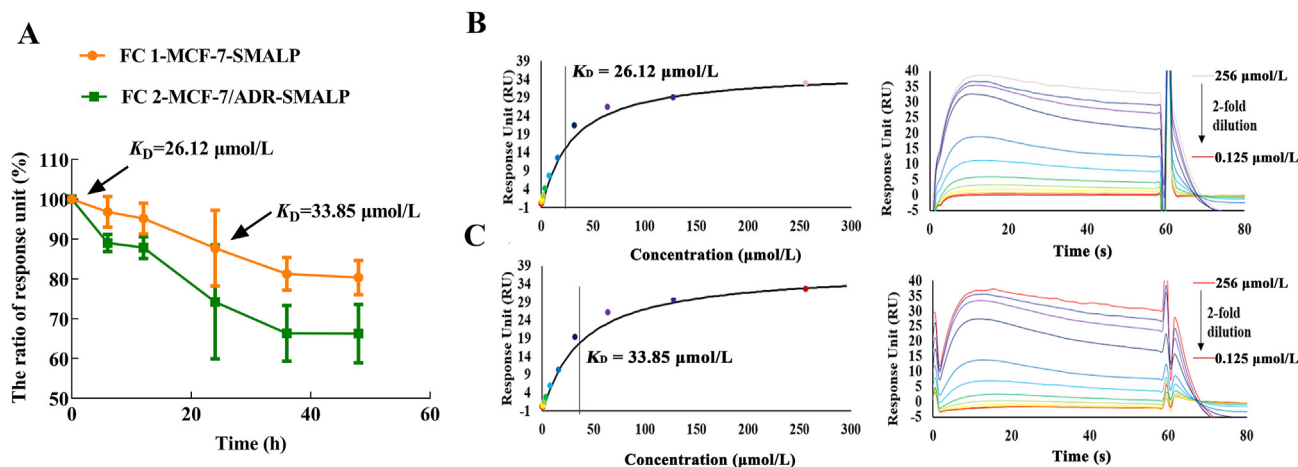


**Figure 6** (A) The stability of SMALPs-MCF-7 and SMALPs-MCF-7/ADR on different channels of the L1 chip (0–48 h), data are mean  $\pm$  SD,  $n = 3$ . The affinity between valsopodar and P-gp after (B) 0 h and (C) 24 h that P-gp-SMALPs-L1 protein chip was established.

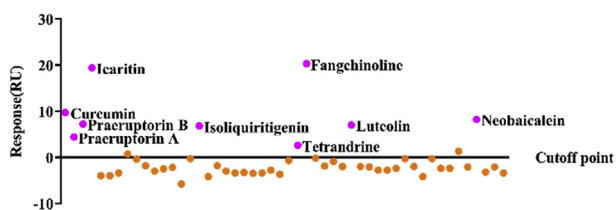


**Figure 7** The response of 50 natural products on the chip. Each point in the figure represents a compound. The pink dot in the figure suggests that the compound may bind to the protein on the chip's surface, while the yellow dot does not respond to the chip.

dexamethasone as a negative drug. It was found that valsopodar and verapamil could bind to the chip, while the negative drug dexamethasone did not respond (Fig. 5B). Similarly, the P-gp specific antibody C494 could bind to the chip (Fig. 5C), which indicated that the constructed analysis method had good specificity and could be used to screen P-gp small molecule ligands. The above results also proved the SMA polymer could keep P-gp in endogenous membrane environment and ensure the correct conformation of P-gp and the accuracy of drug screening.

### 3.7. The stability of P-gp-SMALPs-L1 chip

The surface of L1 chip is dextran matrix, which can covalently combine with lipophilic alkyl groups as active groups. The whole liposome will be captured by lipophilic group, but will not covalently bind to the L1 chip surface. During the usage, the liposomes will detach from the chip, and the protein will also lose its activity. Therefore, it is necessary to investigate the stability of P-gp contained in SMALPs. SMALPs-MCF-7 and SMALPs-MCF-7/ADR were coupled to FC 1 and FC 2 of L1 chip. The absolute response of the chip was recorded at 6, 12, 24 and 48 h, and the loss percentage of SMALPs on the chip at each time point was calculated based on the amount of SMALPs coupled on the channel. The results were shown in Fig. 6A, the content of SMALPs on the two channels gradually decreased with time went by. After 24 h, FC 1 and FC 2 decreased to 85% and 75%, respectively. After 48 h, FC 1 and FC 2 decreased to 80% and 65%, respectively. In order to verify the stability of P-gp in SMALPs, the P-gp-L1 chip's activity was tested with the positive drug after SMALPs coupled and 24 h later by kinetic experiments. The results are shown in Fig. 6B and C. 24 h after coupling, the positive drug had good affinity with P-gp on the chip and the  $K_D$  was 33.85  $\mu\text{mol/L}$ . This indicated that the P-gp on the chip was stable and active within 24 h. The stability results suggested that activity of P-gp-SMALPs-L1 chip can keep 24 h at least, thus, all assays in this study were carried out within 24 h after the SMALPs coupled on L1 chip to ensure the accuracy of the analysis.

### 3.8. Potential P-gp inhibitors screening

Fifty natural products (detailed in Supporting Information) which may relate to P-gp were collected and screened by the system. Compounds were injected into the system one by one, and the analysis time of each compound was about 60 s. As a result, 9 compounds with remarkable response values were regarded as target compounds which could bind to P-gp (Fig. 7). They were tetrandrine, praeruptorin B, fangchinoline, neobaicalein, icaritin, praeruptorin A, luteolin, curcumin and isoliquiritigenin.

Current P-gp screening methods mainly depend on traditional cell experiments and generally take several days. In this study, the developed novel SPR screening system can shorten the time to several hours, greatly improves screening efficiency and has good specificity for P-gp interaction. The small molecule binding sites of P-gp are primarily located in the intracellular domain, and a few binding sites are located in the extracellular domain<sup>32,33</sup>. SMA polymer can be inserted into the cell membrane to form P-gp-SMALPs, and the P-gp stabilized in SMALPs is non-directional, so the developed P-gp-SMALPs SPR screening system can obtain more potential ligands bound to intracellular and extracellular sites.

The LVPs-SPR screening system established in our previous research targeted the binding sites of the extracellular segment of P-gp with fewer ligands obtained because P-gp was integrated into the surface of LVPs envelope<sup>11,12</sup>. Moreover, obtaining SMA polymers is more convenient than constructing and purifying LVPs, and SMA polymer is easy-to-use and inexpensive, and L1 chip can be reused. It is worth noting protein stabilization in SMALPs is also non-directional, and how to extract MPs directionally is necessary to be considered in the future development of MPs ligand screening.

Compared with other MPs stabilization technologies, including liposomes, the whole process of SMA polymer MPs stabilization does not require the participation of detergents, and can avoid loss of protein activity in nano-disc recombination. However, the disadvantage of SMALPs screening system is that the pH dependency of SMA polymer, which makes it incompatible with CM5 chips commonly used. At the same time the pH dependency is also a potential drawback for certain classes of proteins whose function depends on pH.

### 3.9. Affinity determination

The affinity between compounds and the protein were further determined by the SPR analysis system. The 9 target compounds were diluted to different concentrations and injected into the system. The results are shown in Table 2 and Supporting Information Fig. S1. Generally, the affinity detection is considered to be compliant when  $\text{Chi}^2$  values are less than 1/10 of the  $R_{\text{max}}$  value. Smaller  $K_D$  value indicates the stronger binding of the compound to the target protein.  $R_{\text{max}}$  represents the analyte binding capacity which gives an indication of the theoretical analyte binding capacity of the surface. The result showed that valsopodar and 9 target compounds had good affinity with P-gp, which demonstrated the feasibility of the developed method. In the process of Adr inducing drug resistance in MCF-7 cells, P-gp overexpression is usually dominant and other MDR-related resistant proteins besides P-gp might have little influence on the screening of P-gp inhibitors. The

**Table 2** Parameters of affinity determination for nine target compounds.

Compd.	$K_D$ ( $\mu\text{mol/L}$ )	$R_{\text{max}}$ (RU)	$\text{Chi}^2$ (RU <sup>2</sup> )
Tetrandrine	220.6	11.24	0.0178
Fangchinoline	115.9	24.92	0.0346
Curcumin	152.5	270.2	3.88
Luteolin	51.74	47.21	4.43
Neobaicalein	126.8	89.01	9.47
Isoliquiritigenin	255.1	114	0.122
Icaritin	2.546	13.86	0.491
Praeruptorin A	7.175	2.618	0.0329
Praeruptorin B	0.5422	3.498	0.0554



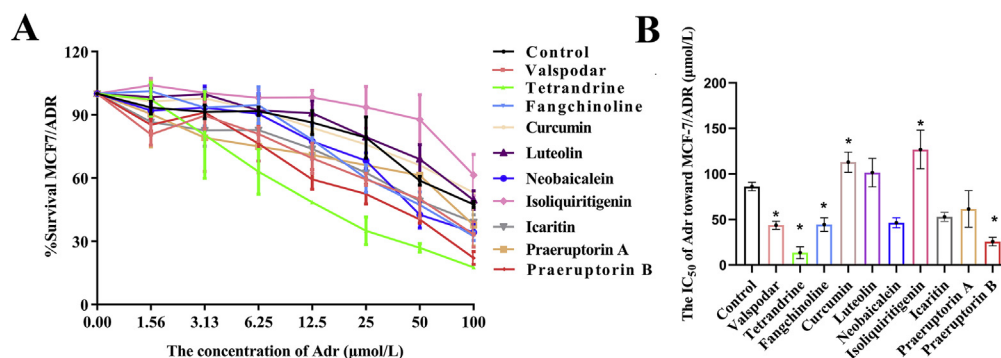


**Figure 8** The activity of potential P-gp inhibitors for reversing MDR of MCF-7/ADR cells (data are mean  $\pm$  SD,  $n = 3$ ;  $*P < 0.05$ , vs. Control). The effect of Adr on MCF-7/ADR cell viability after treatment with the positive drug valspodar and 9 target compounds (A) and the corresponding  $IC_{50}$  value (B).

**Table 3** The bidirectional  $P_{app}$  values and ER of Rh123 in the MDCK-MDR1 cell monolayer treated by different compounds.

Group	Control		Valspodar		Tetrandrine		Fangchinoline		Praeruptin B		Neobaicalein	
	AP-BL <sup>a</sup>	BL-AP	AP-BL	BL-AP	AP-BL	AP-BL	BL-AP	BL-AP	AP-BL	BL-AP	AP-BL	BL-AP
$P_{app}$ ( $\times 10^{-6}$ cm/s)	1.85	5.64	2.42	2.57	1.97	2.85	1.95	3.71	1.98	2.07	1.97	2.30
ER	2.99		1.06*		1.46*		1.89		1.14*		1.38*	

<sup>a</sup> $P_{app}$  (AP-BL) means the apparent permeability of apical to basolateral (AP-BL),  $P_{app}$  (BL-AP) means the apparent permeability of basolateral to apical (BL-AP),  $n = 3$ ,  $*P < 0.05$ , vs. Control.

affinity verification results of the potential target compounds demonstrated the compounds were bound to P-gp and the system was specific for P-gp inhibitor screening.

### 3.10. The reversal effect of target compounds on MDR of MCF-7/ADR cells

Next, the biological activity of the 9 compounds was determined, as well as their activity to reverse MDR *in vitro*. Before verifying the reversal of MDR activity, the maximum non-toxic concentration of each compound was determined using CCK8 assay. The concentrations of 9 compounds were illustrated in Supporting Information Figs. S3–S5, with 95% cell activity as the highest non-toxic concentration. Then,  $IC_{50}$  value of Adr on MCF-7/ADR cells was measured to characterize the reversal of MDR activity by pre-incubating each non-toxic concentration of 9 target compounds with MCF-7/ADR cells for 24 h. The sensitivity of MCF-7/ADR cells to Adr was significantly increased by tetrandrine, praeruptorin B, fangchinoline, neobaicalein, icaritin, and positive drug valspodar (Fig. 8A).

The  $IC_{50}$  of Adr toward MCF-7/ADR after pre-incubating with target compounds are shown in Fig. 8B. The Adr toward MCF-7/ADR were  $13.52 \pm 0.63$ ,  $25.78 \pm 1.62$ ,  $44.43 \pm 7.51$ ,  $46.38 \pm 5.54$ , and  $52.91 \pm 5.07$   $\mu\text{mol/L}$  with treatment of tetrandrine, praeruptorin B, fangchinoline, neobaicalein, and icaritin, respectively, which were lower than control that without treatment of compounds ( $86.09 \pm 4.74$   $\mu\text{mol/L}$ ). Therefore, these results indicated tetrandrine, praeruptorin B, fangchinoline, neobaicalein, and icaritin could reverse the MDR of MCF-7/ADR cells. On the other hand, the Adr toward MCF-7/ADR were  $112.85 \pm 11.13$  and  $126.77 \pm 21.24$   $\mu\text{mol/L}$  with treatment curcumin and isoliquiritigenin, respectively. The results suggested that the two compounds could not improve the sensitivity of Adr toward MCF-7/ADR cells and reverse the MDR. In the previous screening

results, the  $R_{max}$  of curcumin and isoliquiritigenin were larger, which suggested that there might be nonspecific bindings. The activity verification results also demonstrated the specificity of the SPR analysis system.

### 3.11. Effects of active compounds on P-gp-mediated Rh123 transport in MDCK-MDR1

Then Rh123 transport experiment was conducted to investigate the effect of tetrandrine, praeruptorin B, fangchinoline, neobaicalein, and valspodar on P-gp function in MDCK-MDR1 cells. Rh123, a substrate for P-gp, has been widely used as an indicator for testing the activity of P-gp. The  $P_{app}$  and efflux rate (ER) were shown in Table 3 and Fig. 9, which indicated the permeability of Rh 123 and reflected the function of P-gp. In this study, we found that after pre-incubation with valspodar, tetrandrine, praeruptorin B and neobaicalein, the  $P_{app}$  (BL-AP) of Rh123 in MDCK-MDR1 cell decreased and  $P_{app}$  (AP-BL) increased, indicating that they could

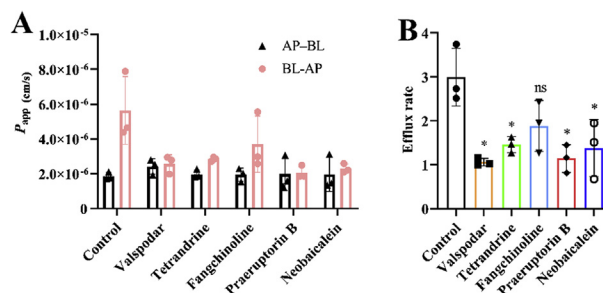


**Figure 9** The effect of positive drug valspodar and active compounds on the bidirectional  $P_{app}$  values (A) and ER (B) of Rh123 in the MDCK-MDR1 cell monolayer (data are mean  $\pm$  SD,  $n = 3$ ,  $*P < 0.05$ , ns, not significant. vs. Control).

significantly reduce the ER of Rh123 and inhibit the function of P-gp. It has been reported that tetrandrine can increase the accumulation of anticancer drugs in MCF-7/ADR cells<sup>34</sup>. Fanchinoline exhibits significant synergistic cytotoxicity when Caco-2 and CEM/ADR cancer cells are co-treated with Adr<sup>35</sup>. The activity verification results were consistent with these reports and demonstrated the reliability of the established P-gp-SMALPs-SPR screening method. Interestingly, neobaicalein and praeruptorin B were reported to reverse MDR in MCF-7/ADR cells for the first time, and their reversal mechanism were also investigated. The Western blot results demonstrated that these compounds did not affect P-gp expression in cancer cells (Fig. S5), indicating that the reversal mechanism of these compounds was by inhibiting the function of P-gp.

#### 4. Conclusions

In this study, we developed an MPs-small molecular ligands SPR analysis system based on SMA polymer MPs stabilization technology. This P-gp-SMALPs-SPR screening system can determine the affinity between compounds and P-gp, allowing for rapid screening of active compounds for MDR reversal. Nine P-gp ligands were screened out by this system from 50 natural products, and their affinity constants towards P-gp were determined. *In vitro* cell verification experiments revealed that tetrandrine, fangchinoline, praeruptorin B, neobaicalein, and icariin could significantly increase the sensitivity of MCF-7/ADR cells to Adr. Tetrandrine, praeruptorin B and neobaicalein were revealed that can reverse the MDR of MCF-7/ADR cells by inhibiting the function of P-gp. In one word, for the first time, SMA-based MPs stabilization technology has been applied to SPR analysis, providing an effective approach for drug screening and affinity detection of complex MPs.

#### Acknowledgments

This research was supported by the National Natural Science Foundation of China (No. 82173777,81872829,81673386,82174092) and the Science and Technology Commission of Shanghai Municipality (21ZR1483000).

#### Author contributions

Study conception and design: Yuhong Cao, Jiahao Fang, Yan Cao and Zhanying Hong; Acquisition, analysis and/or interpretation of data: Yuhong Cao, Jiahao Fang, Yiwei Shi, Hui Wang, Xiaofei Chen; Drafting/revision of the work for intellectual content and context: Yuhong Cao, Jiahao Fang, Yue Liu, Yan Cao and Zhanying Hong; Critical review of the manuscript: Zhenyu Zhu, Yan Cao, Zhanying Hong, Yifeng Chai.

#### Conflicts of interest

The authors declare no competing financial interest.

#### Appendix A. Supporting information

Supporting data to this article can be found online at <https://doi.org/10.1016/j.apsb.2022.03.016>.

#### References

- Inada M, Kinoshita M, Sumino A, Oiki S, Matsumori N. A concise method for quantitative analysis of interactions between lipids and membrane proteins. *Anal Chim Acta* 2019;**1059**:103–12.
- Chen L, Lv D, Chen X, Liu M, Wang D, Liu Y, et al. Biosensor-based active ingredients recognition system for screening STAT3 ligands from medical herbs. *Anal Chem* 2018;**90**:8936–45.
- Maynard JA, Lindquist NC, Sutherland JN, Lesuffleur A, Warrington AE, Rodriguez M, et al. Surface plasmon resonance for high-throughput ligand screening of membrane-bound proteins. *Bio-technol J* 2009;**4**:1542–58.
- Arul Prakash S, Kamlekar RK. Function and therapeutic potential of *N*-acyl amino acids. *Chem Phys Lipids* 2021;**239**:105114–22.
- Hu Q, Su H, Li J, Lyon C, Tang W, Wan M, et al. Clinical applications of exosome membrane proteins. *Precis Clin Med* 2020;**3**:54–66.
- Várady G, Cserepes J, Németh A, Szabó E, Sarkadi B. Cell surface membrane proteins as personalized biomarkers: where we stand and where we are headed. *Biomarkers Med* 2013;**7**:803–19.
- Bocquet N, Kohler J, Hug MN, Kuszniir EA, Rufer AC, Dawson RJ, et al. Real-time monitoring of binding events on a thermostabilized human A2A receptor embedded in a lipid bilayer by surface plasmon resonance. *Biochim Biophys Acta* 2015;**1848**:1224–33.
- Segala E, Errey JC, Fiez-Vandal C, Zhukov A, Cooke RM. Biosensor-based affinities and binding kinetics of small molecule antagonists to the adenosine A(2A) receptor reconstituted in HDL like particles. *FEBS Lett* 2015;**589**:1399–405.
- Aristotelous T, Hopkins AL, Navratilova I. Surface plasmon resonance analysis of seven-transmembrane receptors. *Methods Enzymol* 2015;**556**:499–525.
- Parmar MJ, Lousa Cde M, Muench SP, Goldman A, Postis VL. Artificial membranes for membrane protein purification, functionality and structure studies. *Biochem Soc Trans* 2016;**44**:877–82.
- Chen L, Lv D, Wang S, Wang D, Chen X, Liu Y, et al. Surface plasmon resonance-based membrane protein-targeted active ingredients recognition strategy: construction and implementation in ligand screening from herbal medicines. *Anal Chem* 2020;**92**:3972–80.
- Cao Y, Cao Y, Shi Y, Cai Y, Chen L, Wang D, et al. Surface plasmon resonance biosensor combined with lentiviral particle stabilization strategy for rapid and specific screening of P-glycoprotein ligands. *Anal Bioanal Chem* 2021;**413**:2021–31.
- Knowles TJ, Finka R, Smith C, Lin YP, Dafforn T, Overduin M. Membrane proteins solubilized intact in lipid containing nanoparticles bounded by styrene maleic acid copolymer. *J Am Chem Soc* 2009;**131**:7484–5.
- Esmaili M, Tancowny BP, Wang X, Moses A, Cortez LM, Sim VL, et al. Native nanodiscs formed by styrene maleic acid copolymer derivatives help recover infectious prion multimers bound to brain-derived lipids. *J Biol Chem* 2020;**295**:8460–9.
- Logez C, Damian M, Legros C, Dupré C, Guéry M, Mary S, et al. Detergent-free isolation of functional G protein-coupled receptors into nanometric lipid particles. *Biochemistry* 2016;**55**:38–48.
- Gulamhussein AA, Uddin R, Tighe BJ, Poyner DR, Rothnie AJ. A comparison of SMA (styrene maleic acid) and DIBMA (di-isobutylene maleic acid) for membrane protein purification. *Biochim Biophys Acta Biomembr* 2020;**1862**:183281–9.
- Tanaka M, Miyake H, Oka S, Maeda S, Iwasaki K, Mukai T. Effects of charged lipids on the physicochemical and biological properties of lipid-styrene maleic acid copolymer discoidal particles. *Biochim Biophys Acta Biomembr* 2020;**1862**:183209–16.
- Gulati S, Jamshad M, Knowles TJ, Morrison KA, Downing R, Cant N, et al. Detergent-free purification of ABC (ATP-binding-cassette) transporters. *Biochem J* 2014;**461**:269–78.
- Dörr JM, Koorengel MC, Schäfer M, Prokofyev AV, Scheidelaar S, van der Crujisen EA, et al. Detergent-free isolation, characterization, and functional reconstitution of a tetrameric K<sup>+</sup> channel: the power of native nanodiscs. *Proc Natl Acad Sci U S A* 2014;**111**:18607–12.

20. Paulin S, Jamshad M, Dafforn TR, Garcia-Lara J, Foster SJ, Galley NF, et al. Surfactant-free purification of membrane protein complexes from bacteria: application to the staphylococcal penicillin-binding protein complex PBP2/PBP2a. *Nanotechnology* 2014;**25**: 285101–8.
21. Jamshad M, Charlton J, Lin YP, Routledge SJ, Bawa Z, Knowles TJ, et al. G-protein coupled receptor solubilization and purification for biophysical analysis and functional studies, in the total absence of detergent. *Biosci Rep* 2015;**35**:1–10.
22. He J, Fortunati E, Liu DX, Li Y. Pleiotropic roles of ABC transporters in breast cancer. *Int J Mol Sci* 2021;**22**:3199–221.
23. Chen Z, Shi T, Zhang L, Zhu P, Deng M, Huang C, et al. Mammalian drug efflux transporters of the ATP binding cassette (ABC) family in multidrug resistance: a review of the past decade. *Cancer Lett* 2016;**370**:153–64.
24. Leopoldo M, Nardulli P, Contino M, Leonetti F, Luurtsema G, Colabufo NA. An updated patent review on P-glycoprotein inhibitors (2011–2018). *Expert Opin Ther Pat* 2019;**29**:455–61.
25. Al-Majdoub ZM, Achour B, Couto N, Howard M, Elmorsi Y, Scotcher D, et al. Mass spectrometry-based abundance atlas of ABC transporters in human liver, gut, kidney, brain and skin. *FEBS Lett* 2020;**594**:4134–50.
26. Yang L, Lin IH, Ting CT, Tsai TH. Modulation of the transport of valproic acid through the blood–brain barrier in rats by the *Gastrodia elata* extracts. *J Ethnopharmacol* 2021;**278**:114276–85.
27. Li H, Krstin S, Wink M. Modulation of multidrug resistant in cancer cells by EGCG, tannic acid and curcumin. *Phytomedicine* 2018;**50**: 213–22.
28. Vilar S, Sobarzo-Sánchez E, Uriarte E. *In silico* prediction of P-glycoprotein binding: insights from molecular docking studies. *Curr Med Chem* 2019;**26**:1746–60.
29. Liu Y, Liu R, Yang F, Cheng R, Chen X, Cui S, et al. MiR-19a promotes colorectal cancer proliferation and migration by targeting TIA1. *Mol Cancer* 2017;**16**:53–70.
30. Agarwal S, Sane R, Ohlfest JR, Elmquist WF. The role of the breast cancer resistance protein (ABCG2) in the distribution of sorafenib to the brain. *J Pharmacol Exp Therapeut* 2011;**336**:223–33.
31. Bada Juarez JF, Harper AJ, Judge PJ, Tonge SR, Watts A. From polymer chemistry to structural biology: the development of SMA and related amphipathic polymers for membrane protein extraction and solubilisation. *Chem Phys Lipids* 2019;**221**:167–75.
32. Pan X, Mei H, Qu S, Huang S, Sun J, Yang L, et al. Prediction and characterization of P-glycoprotein substrates potentially bound to different sites by emerging chemical pattern and hierarchical cluster analysis. *Int J Pharm* 2016;**502**:61–9.
33. Globisch C, Pajeva IK, Wiese M. Identification of putative binding sites of P-glycoprotein based on its homology model. *ChemMedChem* 2008;**3**:280–95.
34. Jiang M, Zhang R, Wang Y, Jing W, Liu Y, Ma Y, et al. Reduction-sensitive paclitaxel prodrug self-assembled nanoparticles with tetrandrine effectively promote synergistic therapy against drug-sensitive and multidrug-resistant breast cancer. *Mol Pharm* 2017;**14**:3628–35.
35. Sun YF, Wink M. Tetrandrine and fangchinoline, bisbenzylisoquinoline alkaloids from *Stephania tetrandra* can reverse multidrug resistance by inhibiting P-glycoprotein activity in multidrug resistant human cancer cells. *Phytomedicine* 2014;**21**:1110–9.